Surface reactions of nitrogen oxide and ethylene on rhodium(111)

Please check the document version of this publication:

Surface reactions of nitrogen oxide and ethylene on rhodium (111)

R.M. van Hardeveld, A.J.G.W. Schmidt and J.W. Niemantsverdriet [a,1]

Schuit Institute of Catalysis, Eindhoven University of Technology, 5600 MB, The Netherlands
[a] E-mail: tgtahn@chem.tue.nl

Temperature programming of NO and C_2H_4 coadsorbed on Rh(111) gives rise to the desorption of a number of gases. Where H_2, H_2O, CO_2 and N_2 are the main products at low C_2H_4 coverages, significant amounts of HCN, CO and NO evolve at higher C_2H_4 coverages. Static SIMS indicates the formation of a large supply of adsorbed CN species, part of which desorbs as HCN, while the remainder decomposes and is responsible for delayed formation of N_2. For the highest C_2H_4 coverages the majority of the initially adsorbed NO desorbs as HCN.

Keywords: NO reduction; TPRS; SIMS; ethylene; rhodium

1. Introduction

Although the reaction between NO and CO to CO_2 and N_2 is commonly held responsible for the removal of NO from automotive exhausts on the three-way catalyst, hydrogen and hydrocarbons make a substantial contribution to NO reduction as well [1]. Cracking of gasoline in the engine of a car is the source of H_2 (estimated to account for roughly 30% of the concentration of CO in the exhaust) and a range of smaller hydrocarbons, among which methane, acetylene, ethylene, benzene and toluene are the most abundant ones [2]. Unsaturated hydrocarbons such as ethylene and propylene readily adsorb on the noble metals of the three-way catalyst and are a source of H- and C-atoms available for reaction with e.g. the O-atoms of dissociatively adsorbed NO and O_2.

Several papers are available on the reduction of NO by small hydrocarbons in copper exchanged zeolites [3–5], but much less is known about their interaction on platinum and rhodium [6]. A recent infrared study by Bamwenda et al. [7] revealed that the surface of a Rh/Al_2O_3 catalyst contained NCO and CN species during the selective reduction of NO by propylene. This is illustrative for a rather rich surface chemistry, allowing for several possible reaction pathways in which the formation of undesired products, such as HCN, HCNO, NH_3 [8,9] or even NH_4OCN [10], is conceivable. Delouise and Winograd investigated the reactions between NO and carbon on Rh(331) by XPS and SIMS and detected a CN surface species in the temperature range between 400 and 800 K [11]. Harkness and Lambert recently reported on an electrochemical promotion effect of Na on the reaction between NO and C_2H_4 on Pt, assigned to enhanced NO dissociation [12].

In this paper we use temperature programmed reac-

tion spectroscopy (TPRS) and secondary ion mass spectrometry (SIMS) to explore the surface reactions between NO and C_2H_4 on rhodium (111). The adsorption of each of these gases separately on Rh(111) is well documented in work from several laboratories [13–16].

2. Experimental

The experiments were done in a UHV system (base pressure around 10^{-10} mbar) equipped with a Leybold SSM 200 quadrupole mass spectrometer for TPD and SSIMS measurements, as described in detail elsewhere [14]. The rhodium crystal, cut in the [111] orientation within 0.5° and polished by standard procedures, was mounted on a moveable stainless steel manipulator with 0.3 mm thick tantalum wires, where it could be cooled to liquid nitrogen temperature and resistively heated up to 1500 K. Temperatures were measured with a chromel-alumel thermocouple spotwelded on the backside of the crystal. Small amounts of bulk impurities, such as sulphur, chlorine, and boron, were removed by cycli of argon sputtering (1.5 keV, 5 $\mu A/cm^2$) at 900 K and annealing to 1400 K. Carbon was removed by annealing the crystal in 2×10^{-8} mbar O_2, by slowly varying the temperature between 900 and 1100 K. Oxygen was removed from the surface by annealing shortly to 1425 K. Ethylene (Messer Griesheim, 99.95% pure) was used without further purification; gas exposures are reported in langmuir (1 L = 1.33×10^{-6} mbar s); coverages are reported in monolayers (ML, number of adsorbates per Rh surface atom).

3. Results and discussion

First we briefly describe the most important characteristics of the adsorption and decomposition of ethylene

---

[1] To whom correspondence should be addressed.

and NO separately on Rh(111). Next follows a qualitative description of the reactions and surface species during heating of coadsorbed NO and ethylene on the basis of TPD and SIMS measurements. Finally, we discuss the influence of the amount of coadsorbed ethylene on the product distribution on the basis of oxygen and nitrogen mass balances.

3.1. NO on Rh(111)

The dissociative adsorption of NO on Rh(111) and the selectivity towards formation of N_2 are strongly affected by the extent to which the surface is occupied [13]. Fig. 1a shows a few TPD spectra of characteristic cases. At low NO coverages (below 0.2 ML), all NO dissociates, and N_2, labelled β_2-N_2 is seen to desorb between 500 and 700 K. SIMS measurements indicated that all NO dissociated already around room temperature, hence β_2-N_2 evolution is a fully desorption limited process.

If the NO coverage is higher than about 0.2 ML, part of the NO desorbs, and N_2 desorbs in two states, a low temperature state indicated as β_1-N_2, which shows first-order desorption kinetics and comes just after the desorption of the NO, and the normal second-order desorption channel of β_2-N_2, which, however, is strongly affected by repulsive interactions with N- and O-atoms [13]. SIMS experiments showed that NO dissociation is retarded to temperatures where NO desorption takes place.

This coverage-dependent effect in the dissociation rate of NO has been attributed to an ensemble requirement of a dissociating NO molecule [13,17]. As a result, the dissociation at fully occupied surfaces is retarded to the temperatures where NO desorbs, after which dissociation of NO and desorption of β_1-N_2 follow instantaneously.

3.2. C_2H_4 on Rh(111)

Decomposition of olefins such as ethylene and propylene has extensively been studied on Pt and Rh [14–16,18,19]. In brief, ethylene adsorbs molecularly on rhodium at low temperatures, say around 120 K, and at around 180 K it reacts to a species called ethylidyne, CCH_3, and a H-atom. Around 300 K the ethylidyne decomposes further to acetylide (CCH), CH and carbidic C-atoms [19]. The decomposition reaction is retarded at higher coverages. Fig. 1b shows the evolution of H_2 during the decomposition. Up to 0.25 ML, all ethylene decomposes and H_2 is the only product observed in the gas phase. At higher coverages, the excess ethylene desorbs, mainly at 180 K [14]. Note that at these higher coverages, hydrogen continues to be present in the form of CH_x species to temperatures as high as 700 K, as fig. 1b shows.

The conversion of ethylene to ethylidyne on Rh(111) has been followed in situ with static SIMS. For low coverages of ethylene (around 0.05 ML), evidence was found that the reaction proceeds through a vinyl ($-CH=CH_2$) intermediate [14]. This in contrast to the situation on Pt(111), where ethylidene, $=CH-CH_3$, has
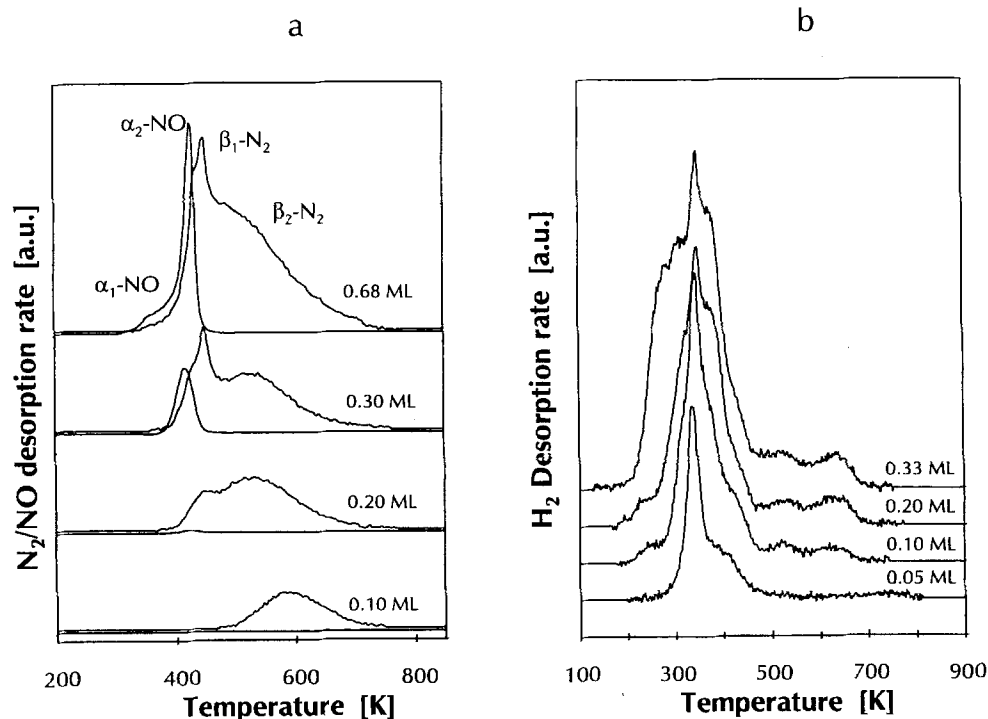
a

b

Fig. 1. (a) Temperature programmed desorption of N_2 and NO from a Rh(111) surface covered with the indicated amounts of NO (heating rate 10 K/s), and (b) TPD of H_2 from ethylene on Rh(111). The adsorption temperature was 100 K, and the heating rate 5 K/s.

been proposed as the intermediate towards ethylidyne [20].

3.3. Coadsorption of NO and ethylene

We now turn to coadsorbed NO and C_2H_4, and use the TPD/TPSIMS experiment performed on 0.20 ML of NO coadsorbed with 0.12 ML of ethylene in fig. 2 to illustrate qualitatively which reaction pathways occur.

The TPD spectra in the upper half of fig. 2 confirm that NO and ethylene not only react to the products that are desirable in the context of automotive exhaust catalysis, N_2, CO_2 and H_2O, but in addition one also observes significant amounts of H_2, NO, CO, and HCN. The signal at 28 amu can be due to three different molecules, ethylene, CO and N_2. However, following the proper fragmentation signals at 12, 14, 16 and 27 amu enables one to distinguish between all three (and HCN, which also comes at 27 amu). It appears that ethylene does not desorb in this particular experiment, that the

peaks between 400 and 600 K are due to CO and that the peak above 700 K is caused by desorption of N_2.

In order to obtain information on the processes occurring on the surface during heating, we have applied static SIMS, see the lower half of fig. 2. As the number of mass channels that can be measured simultaneously is limited, we only report a few characteristic secondary ions, such as $RhC_2H_4^+$ representing molecularly adsorbed C_2H_4, $RhCO^+$ for adsorbed CO, Rh_2C^+ and Rh_2N^+ for adsorbed C- and N-atoms, Rh_2CN^+ for adsorbed cyanide groups, and CH_3^+, which is characteristic for the ethylidyne species, CCH_3 [14,21]. In order to compensate at least partially for effects due to changes in work function during decompositions and reactions on the surface, it is customary to consider intensity ratios such as $RhC_2H_4^+/Rh^+$, which often quite closely correlate with adsorbate coverage [22,23].

At low temperature, both NO and C_2H_4 adsorb molecularly. The ethylene reveals itself in SIMS through a $RhC_2H_4^+$ secondary ion. The first surface reaction that occurs during heating of C_2H_4 and NO is the conversion of ethylene to ethylidyne, CCH_3, and H-atoms, between 190 and 220 K [14]. The SIMS spectra in fig. 2 indicate the conversion of ethylene by a decrease of the $RhC_2H_4^+$ ratio and the accompanied formation of ethylidyne by the appearance of the methyl secondary ion, CH_3^+. The H-atoms formed in the ethylene → ethylidyne reaction start to desorb around 270 K.

Just below 300 K, NO dissociation sets in, as reflected by the growth of the Rh_2N^+ signal characteristic of N-atoms, and the evolution of H_2O, which is reaction limited above 200 K on Rh(111) [24]. NO dissociation occurs in two steps, the first between roughly 300 and 350 K, after which the Rh_2N^+ intensity reaches a short plateau, and the second above 400 K, as can be inferred from a further rise in the Rh_2N^+ intensity and the appearance of additional peaks in the desorption of CO_2 and H_2O, as we discuss in more detail below.

The decomposition of ethylidyne, seen by the decrease of the CH_3^+ intensity in SIMS, falls in the temperature range of approximately 300–380 K, and is accompanied by the formation of H-atoms, which either desorb as H_2 or react with O-atoms and a second H-atom to H_2O, which desorbs instantaneously. H_2 desorption terminates at about 450 K. Note however that the surface still contains hydrogen – most probably present in the form of carbonaceous species – as H_2O and HCN continue to desorb to almost 600 and 700 K, respectively.

Oxidation of C-atoms appears to begin at 380 K, as the growth of a $RhCO^+$ in SIMS, and the more or less simultaneous desorption of CO_2 indicate. Apparently, the reaction between adsorbed CO and O is not sufficiently rapid to prevent the accumulation of CO on the surface. CO desorption is seen above 450 K both in TPD and in SIMS, in agreement with the literature of CO on Rh(111) [25,26]. Also in this region, 450–520 K, is the de-
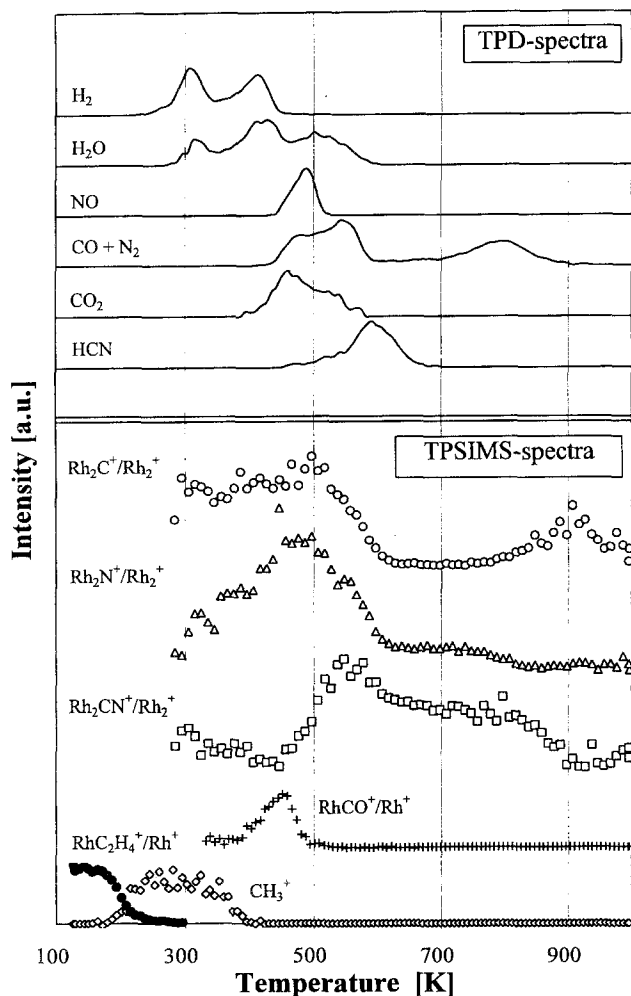

Fig. 2. Temperature programmed reactions of 0.12 ML of ethylene coadsorbed with 0.20 ML of NO as followed by TPD and SIMS (see text for explanation). The adsorption was done at 100 K, and the heating rate was 10 K/s.

sorption of NO. Note that the desorption temperature of NO is significantly (i.e. about 70 K) higher than if NO is the only adsorbate (fig. 1a). Following earlier work, we propose that this NO desorbs because the surface is to a large extent occupied, implying that the relatively large ensembles of free rhodium atoms necessary for NO dissociation are not available [13,17]. Hence, NO desorbs as soon as the temperature is high enough to permit this.

The SIMS data in fig. 2 strongly suggest that a large inventory of cyanide groups forms on the surface between 450 and 550 K. First, the Rh_2CN^+ intensity increases strongly and second, the intensities of both Rh_2N^+ and Rh_2C^+, characteristic of atomic nitrogen and carbon at these temperatures, decrease. Although the Rh_2C^+ is observed as a fragment of adsorbed C_2H_x species as well, it is very likely that all C–C bonds have broken at the temperatures where CN groups start to form (i.e. 450 K). The Rh_2N^+ intensity falls to a low value reflecting the fragmentation of Rh_2CN^+, while the Rh_2C^+ falls practically to zero. Note that the observation of CN on the surface coincides with the onset of the HCN desorption and that CN formation occurs at higher temperatures than CO formation, reflecting that the reaction between carbon and oxygen is preferred above that between carbon and nitrogen atoms.

We do not believe that the cyanide is present as adsorbed HCN, because, first, the SIMS signal of the corresponding Rh_2HCN^+ is not observed and second, the irregular leading edge of the HCN desorption trace suggests a reaction limited desorption process. Part of the cyanide inventory is hydrogenated to HCN between 500 and 650 K, as seen by the desorption of HCN and the decrease in the Rh_2CN^+ SIMS signal. Apparently, the adsorbate layer is fully dehydrogenated above 650 K. The cyanide species remain stable until about 720 K where N_2 desorption starts to occur, as evidenced by the N_2 signal in TPD (accompanied by a parallel signal at 14 amu), a decrease in the Rh_2CN^+ signal in SIMS and an increase in the Rh_2C^+ signal characteristic of adsorbed carbon. The Rh_2N^+ ion characteristic of adsorbed N-atoms, is not observed, indicating that N_2 desorbs instantaneously. The decrease of the Rh_2C^+ signal above 900 K is attributed to the dissolution of carbon into the rhodium crystal [27].

3.4. Coverage dependence

Fig. 3 shows the evolution of the different desorbing gases as a function of increasing ethylene exposure for a fixed coverage of 0.20 ML of NO. The H_2 TPD patterns start similarly as in the ethylene only case, with a desorption limited state at about 310 K, which at low coverages is largely attributed to the recombinative desorption of H-atoms formed at lower temperature (180–220 K) in the ethylene → ethylidyne conversion. The second peak growing in the range of 375–400 K is entirely attributed

to reaction limited desorption of H_2 originating from the decomposition of hydrocarbon fragments. Whereas H_2 desorption continues up to 700 K for high coverages of ethylene in the absence of coadsorbed NO, it now stops at 450 K.

Water desorption occurs in three distinct states. At all coverages, the water signal starts to grow at about 280 K, which is the temperature where NO dissociation is known to begin [13]. Desorption of molecularly adsorbed water from Rh(111) occurs already between 150 and 220 K, as reported by Wagner and Moylan [24]. The second state, with a peak maximum above 400 K, parallels the second H_2 desorption state and the second NO dissociation step (see fig. 2), and is due to recombinative desorption of O-atoms with H-atoms originating from the decomposition of C_xH_y fragments on the surface. Note that the selectivity of the H-atoms generated in this temperature interval (i.e. 350–450 K) to form H_2O is high at initially low ethylene coverage, and decreases when the H-content of the adsorbate layer increases, as expected. Interestingly, a third, reaction limited H_2O desorption state develops around 500–540 K, at high initial ethylene coverages. The intensity of this state parallels that of the NO desorption at somewhat lower temperature. We propose that the NO desorption between 450 and 520 K (which is significantly above the dissociation temperature of NO on the Rh(111) surface), together with the desorption of other gases such as CO and CO_2, create space where additional NO dissociates, thus creating atomic oxygen giving rise to further H_2O formation. As neither H-atoms nor OH groups have a sufficiently long residence time on the surface at these temperatures, we propose that water formation between 500 and 600 K occurs by reactions such as $O_{ads} + CH_{ads} \rightarrow OH_{ads} + C_{ads}$, followed instantaneously by $OH_{ads} + CH_{ads} \rightarrow H_2O + C_{ads}$.

The desorption of NO increases strongly with increasing total coverage, reflecting the ensemble requirement of the NO dissociation. It is interesting to note that the peak maximum temperature of 480–500 K is significantly higher than in the case of NO desorption from a Rh(111) surface occupied by NO only, which occurs at 430 K (see fig. 1a). In the latter case NO may be destabilized by repulsive lateral interactions with NO, N and O, whereas in the present case NO desorbs out of an environment dominated by hydrocarbon fragments together with CO, NO and N, which apparently gives rise to reduced repulsion or possibly even attractive lateral interaction with the NO.

The mass 28 TPD spectra in fig. 3 are mainly due to CO and N_2, and at high initial ethylene coverages probably also to C_2H_4. For intermediate coverages, one recognizes two CO desorption states with peak maximum temperatures of about 475 and 540–550 K. The first is due to the desorption of adsorbed CO, which formed on the surface between 400 and 475 K (see the $RhCO^+$ SIMS signal in fig. 2). The higher occurs almost
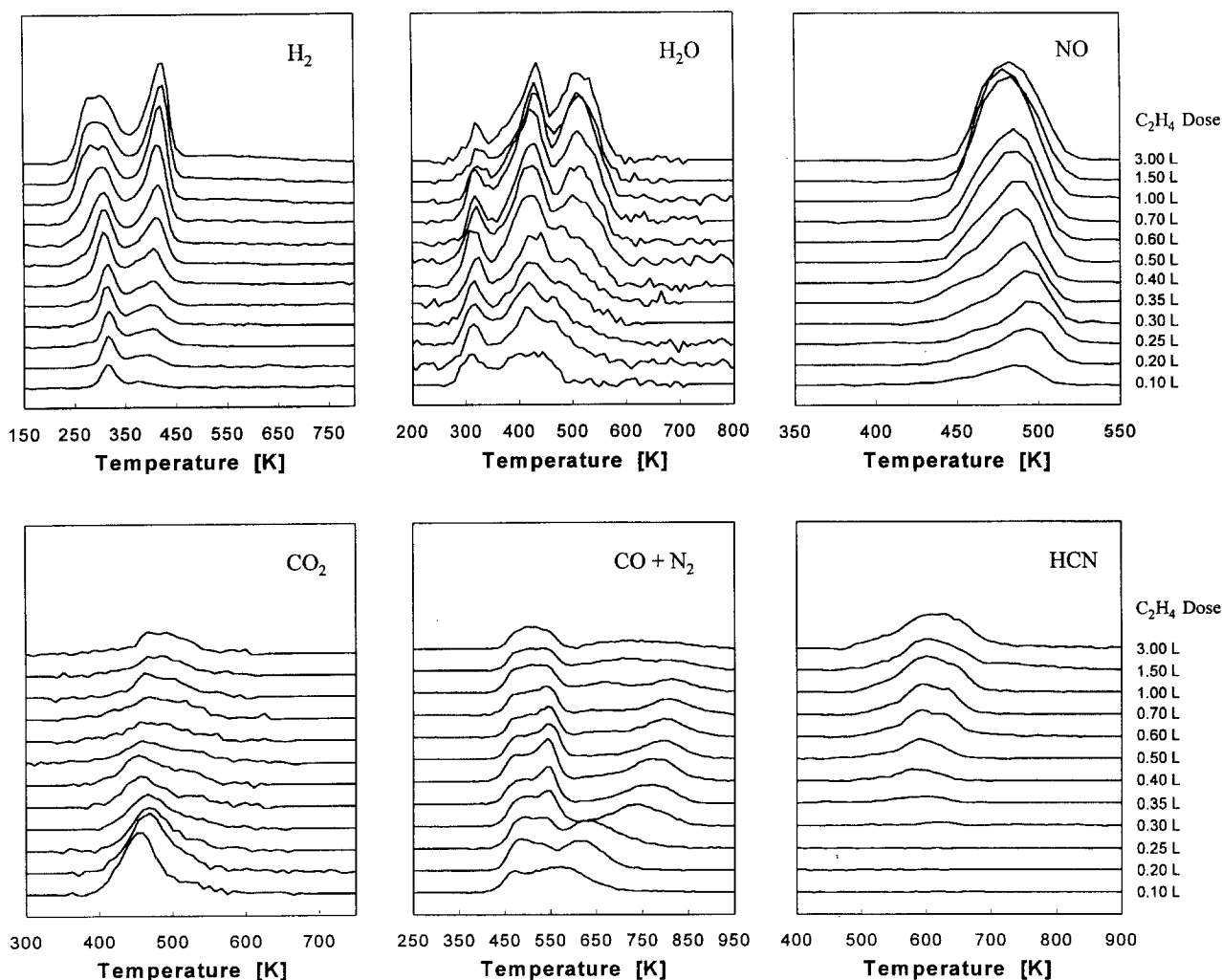
Fig. 3. TPD spectra of 0.20 ML of NO, coadsorbed with varying amounts of ethylene on Rh(111), measured at a heating rate of 10 K/s. The adsorption temperature was 100 K.

simultaneously with the third H_2O desorption state and is attributed to the evolution of O-atoms from additionally dissociating NO molecules at higher temperatures, as discussed above.

CO_2 desorption is seen to commence significantly before CO desorbs, and parallels qualitatively the concentration of adsorbed CO as detected in SIMS (fig. 2). Hence, we conclude that CO_2 desorption is favoured above desorption of CO, but is limited by the availability of adsorbed O-atoms. This is in agreement with the dependence of the CO_2 TPD intensities on both temperature and initial ethylene coverage.

The maximum of the N_2 desorption shifts from 550–600 K at low to above 800 K for high initial ethylene coverage. We propose that the low temperature N_2 desorption is due to recombinative desorption of atomic nitrogen, while the states at higher temperature reflect the decomposition of CN species in the range of 750–900 K (fig. 2), after which N atoms desorb instantaneously in a second-order process. The initial shift of the N_2 desorption peak from 550–600 K upward when

ethylene is coadsorbed in small amounts may well reflect the relieve of repulsive interactions by oxygen atoms that have been removed as H_2O and CO_2 or CO [13]. The further shift of the N_2 signal to higher temperatures, however, is predominantly the effect of CN formation.

Finally, HCN desorption is observed at the higher initial ethylene coverages, i.e. above 0.30 L C_2H_4 exposure. We take the irregularities in the desorption traces as an indication that HCN desorption is a reaction limited process. In principle there are two different reaction routes possible for HCN formation. The first one could be a direct coupling according to $CH_{ads} + N_{ads} \rightarrow HCN\uparrow$. Secondly, HCN could also be formed by the hydrogenation of CN which has previously been formed by the reaction $C_{ads} + N_{ads} \rightarrow CN_{ads}$. In the latter case HCN formation is limited by the availability of H-atoms, e.g. $CH_{ads} \rightarrow C_{ads} + H_{ads}$. It should be noted that if HCN formation proceeds according to the hydrogenation of CN by surface hydrogen, this process is highly favoured above H_2 desorption since the latter is not observed.

3.5. O- and N-mass balances

Fig. 4 shows the mass balances of nitrogen and oxygen, for a fixed coverage of 0.20 ML of NO and C_2H_4 exposures of 0.20 and 0.70 L, representing a low (~ 0.05 ML) and high (~ 0.17 ML) ethylene coverage situation, respectively. For the low coverage case of coadsorbed ethylene, nitrogen preferentially forms N_2, and oxygen CO_2 and H_2O. As the coverage of the "reducing agent" ethylene increases, one sees that the desired reduction of NO becomes increasingly less successful: The selectivity of nitrogen to leave the surface as HCN and NO increases and that of oxygen to form CO_2 decreases significantly.

4. Concluding remarks

Temperature programmed reaction of NO and C_2H_4 produces a broad spectrum of products. At low C_2H_4 coverages, H_2, H_2O, CO_2 and N_2 are the dominant products, but as the coverage increases, NO dissociation becomes hindered, and the fraction of NO that does dissociate has a relatively large probability to be trapped in an extensive reservoir of CN species, which forms between 450 and 550 K. This is well above the NO dissociation temperature on occupied surfaces, and also above the temperature where the C–C bond breaks, hence we conclude that neither NO dissociation nor C–C bond scission are rate determining and that CN formation from adsorbed C and N atoms has an activation barrier which gives rise to a formation temperature above 450 K. Depending on the availability of H-atoms which are released from hydrocarbon fragments in the temperature range of 500–700 K, CN may be hydrogenated to gas phase HCN. In the absence of hydrogen, the CN species are sufficiently stable to retard the desorption of N_2 by some 200 K to the range of 650–850 K.

Preliminary experiments on the reaction between adsorbed N atoms and ethylene have revealed that the selectivity for N to desorb as HCN may be close to 100% [28]. These experiments thus suggest that it should be possible to design a low temperature process for HCN formation starting from NO and ethylene.
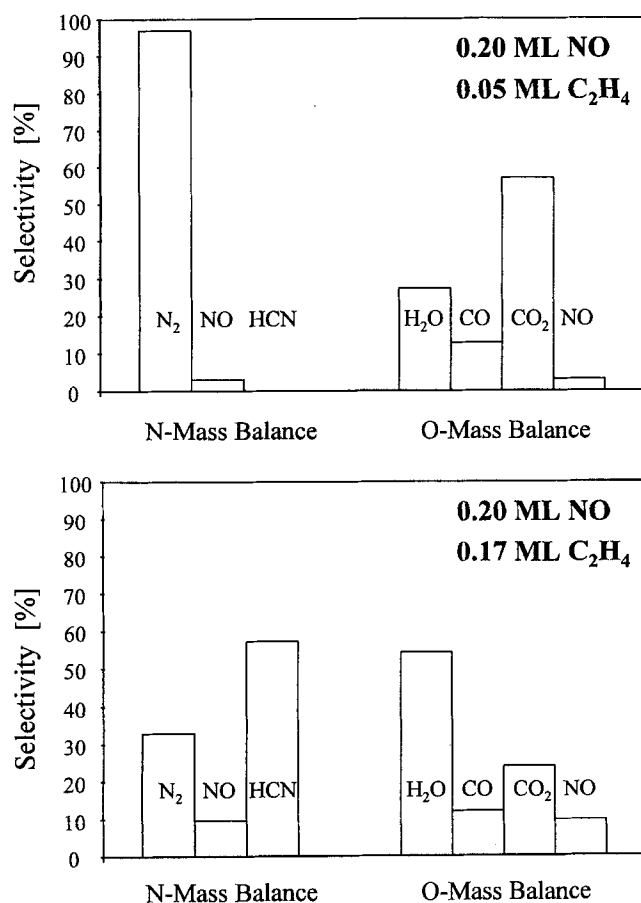
Acknowledgement

Fig. 4. O- and N-mass balances showing the selectivities of N and O atoms from 0.20 ML of NO on Rh(111) to desorb in the form of the indicated gases for a low (~ 0.05 ML) and a high (~ 0.17 ML) ethylene coverage case, obtained by exposing 0.20 and 0.70 L C_2H_4, respectively.

References

[1]   K.C. Taylor, Catal. Rev. Sci. Eng. 35 (1993) 457.
[2]   R. Impens, in: Catalysis and Automotive Pollution Control, eds. A. Crucq and A. Frennet (Elsevier, Amsterdam, 1987) p. 11.
[3]   M. Iwamoto and H. Hamada, Catal. Today 10 (1991) 57.
[4]   J.N. Armor, Catal. Today 26 (1995) 99, and references therein.
[5]   A.P. Walker, Catal. Today 26 (1995) 107.
[6]   R. Burch and P.J. Millington, Catal. Today 26 (1995) 185.
[7]   G.R. Bamwenda, A. Obuchi, A. Ogata and K. Mizuno, Chem. Lett. (1994) 2109.
[8]   C. Yokoyama and M. Misono, J. Catal. 150 (1994) 9.
[9]   F. Radtke, R.A. Köppel and A. Baiker, Catal. Today 26 (1995) 159.
[10] R.J.H. Voorhoeve, C.K.N. Patel, L.E. Trimble and R.J. Kerl, J. Catal. 54 (1978) 102.
[11] L.A. DeLouise and N. Winograd, Surf. Sci. 154 (1985) 79.
[12] I.A. Harkness and R.M. Lambert, J. Catal. 152 (1995) 211.
[13] H.J. Borg, J.F.C.J.M. Reijerse, R.A. van Santen and J.W. Niemantsverdriet, J. Chem. Phys. 101 (1994) 10052.
[14] H.J. Borg, R.M. van Hardeveld, and J.W. Niemantsverdriet, J. Chem. Soc. Faraday Trans. 91 (1995) 3679.
[15] G.A. Somorjai, M.A. Van Hove and B.E. Bent, J. Phys. Chem. 92 (1988) 973.
[16] L.H. Dubois, D.G. Castner and G.A. Somorjai, J. Chem. Phys. 72 (1980) 5234.
[17] R.A. van Santen and J.W. Niemantsverdriet, Chemical Kinetics and Catalysis (Plenum, New York, 1995).
[18] F. Zaera, J. Am. Chem. Soc. 111 (1989) 8744; Acc. Chem. Res. 25 (1992) 260.

[19] G.A. Somorjai, *Introduction to Surface Chemistry and Catalysis* (Wiley, New York, 1994).

[20] P. Cremer, C. Stanners, J.W. Niemantsverdriet, Y.R. Shen and G.A. Somorjai, Surf. Sci. 328 (1995) 111.

[21] J.R. Creighton and J.M. White, Surf. Sci. 129 (1983) 327.

[22] J.W. Niemantsverdriet, *Spectroscopy in Catalysis* (VCH, Weinheim, 1993).

[23] H.J. Borg and J.W. Niemantsverdriet, in: *Catalysis*, Specialist Periodical Report, Vol. 11, eds. J.J. Spivey and A.K. Agarwal (The Royal Society of Chemistry, Cambridge, 1994) p. 1.

[24] F.T. Wagner and T.E. Moylan, Surf. Sci. 191 (1987) 121.

[25] P.A. Thiel, J.T. Yates and W.H. Weinberg, Surf. Sci. 84 (1979) 54.

[26] L.H. Dubois and G.A. Somorjai, Surf. Sci. 91 (1980) 514.

[27] D.G. Castner and G.A. Somorjai, Surf. Sci. 83 (1979) 60.

[28] R.M. van Hardeveld, R.A. van Santen and J.W. Niemantsverdriet, in preparation.